

Band bending and interface states for metals on GaAs

R. E. Viturro, J. L. Shaw, C. Mailhot, and L. J. Brillson
Xerox Webster Research Center, Webster, New York 14580

N. Tache, J. McKinley, and G. Margaritondo
Physics Department, University of Wisconsin-Madison, Wisconsin 53706

J. M. Woodall, P. D. Kirchner, G. D. Pettit, and S. L. Wright
IBM Thomas J. Watson Research Center, Yorktown Heights, New York 10598

(Received 19 February 1988; accepted for publication 14 April 1988)

We have used soft x-ray photoemission and optical emission spectroscopies to observe a broad range of Fermi level stabilization energies at metal interfaces with GaAs(100) surfaces grown by molecular beam epitaxy (MBE). The observed metal- and As-related interface cathodoluminescence plus orders-of-magnitude differences in bulk-defect-related photoluminescence between melt- versus MBE-grown GaAs suggest a role of bulk crystal growth and processing in controlling Schottky barrier formation.

The understanding and control of electrical barriers at metal-semiconductor interfaces has been a major challenge in solid-state physics for several decades.¹ Among III-V compound semiconductors, GaAs is the prime example of this issue since most experimental evidence to date indicates interface Fermi level (E_f) stabilization in a narrow range of band-gap energies, irrespective of the deposited metal.^{2,3} Such experiments form the basis of several physical models which account for the interface E_f "pinning."¹⁻⁶ Recently, we reported several ultrahigh vacuum (UHV) studies on a variety of metal/III-V compound semiconductor interfaces which reveal E_f stabilizations over wide energy ranges. These results for metal/GaP,⁷ InAs,⁸ and $\text{In}_x\text{Ga}_{1-x}\text{As}$ ($0 < x < 1$)⁸ interfaces suggest that the E_f pinning reported for GaAs is not characteristic of III-V compound semiconductors. Non-UHV measurements for GaAs are usually performed on melt-grown materials, i.e., liquid-encapsulated Czochralski (LEC) or horizontal Bridgman (HB)-grown single crystals. Past UHV measurements are based primarily on cleaved, LEC-grown or air-exposed, molecular beam epitaxy (MBE)-grown GaAs surfaces. Crystal quality and bulk trap density vary significantly between these materials, depending on factors which may affect interface charge redistribution. For this reason and since GaAs epilayers are the basis for many future semiconductor applications, we have investigated Schottky barrier and interface state formation for metals deposited on clean, ordered MBE-grown GaAs surfaces. Soft x-ray photoemission spectroscopy (SXPS) results for different metals on MBE-grown GaAs(100) surfaces reveal a much broader range of E_f stabilization energies than hitherto observed. Cathodoluminescence (CLS) and photoluminescence (PLS) spectroscopies provide direct optical evidence for metal-specific,^{6,9} As-related⁴, as well as bulk-defect-related states forming during semiconductor metallization. Indeed, we observe much larger concentrations of midgap bulk defect levels for LEC-grown GaAs, suggesting that semiconductor growth quality is responsible for the difference in interface charge accumulation and the much narrower range of LEC- vs MBE-grown GaAs Schottky barrier heights (SBH). For the lower bulk state

density MBE-grown GaAs, we observe an interplay between these three types of states at the interface.

The MBE specimens have an unstrained, epitaxial overlayer, Ohmic contact layer structure consisting of 7500-Å-thick GaAs ($n = 5 \times 10^{16} - 5 \times 10^{17} \text{ Si/cm}^3$ or $p = 1 \times 10^{18} \text{ Mg/cm}^3$) grown over a 2000 Å GaAs ($n = 2 \times 10^{18} \text{ Si/cm}^3$ or $p = 6 \times 10^{18} \text{ Mg/cm}^3$) on top of an n^+ - or p^+ -GaAs(100) substrate, respectively. Following MBE growth the specimen surfaces were "capped" *in situ* with several hundred angstroms of As as protection against ambient contamination. These caps were thermally desorbed in UHV to provide clean ordered GaAs(100) surfaces, as determined by valence-band (VB) photoemission and low-energy diffraction measurements.⁸ Experimental procedures for the SXPS,⁸ CLS,¹⁰ and PLS¹⁰ measurements appear elsewhere. We evaporated metals from pre-outgassed W sources and monitored deposited thicknesses with a quartz oscillator near the GaAs surface.

Figure 1 shows E_f movements with respect to the GaAs band edges as a function of Au, Al, Cu, and In deposition for

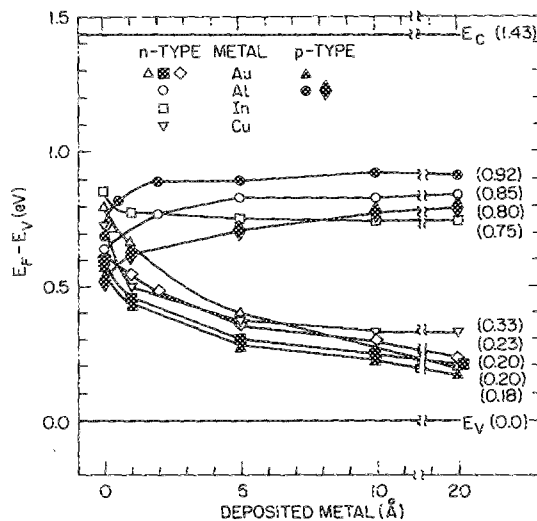


FIG. 1. E_f movements for clean MBE-grown GaAs(100) as a function of Au, Al, In, and Cu deposition.

several *n*- and *p*-type MBE UHV-cleaned GaAs(100) surfaces. The E_f positions of the clean GaAs(100) surfaces were determined by the usual extrapolation of the VB edge versus the E_f of a thick Au film. Three major features are evident. First, the range of E_f stabilization energies extends over 0.6–0.7 eV. Second, the final E_f positions for *n*- and *p*-type specimens converge to the same energy for the same metal in both Au and Al cases. Third, the rate of E_f change depends on the particular metal, and can evolve over 10–20 Å of deposited metal to its final position. All three aspects contrast strongly with similar measurements for UHV-cleaned (LEC) GaAs, where (1) a range of only 0.2 eV is evident, (2) final E_f positions are separated by the same 0.2 eV range, and (3) E_f positions evolve for most metals over submonolayers.² A 0.35-eV-wide E_f band near the conduction band (CB) for MBE-grown GaAs with epitaxial Ge overlayers further supports this “unpinned” E_f ,¹¹ although epitaxial growth at elevated temperatures can produce quite different band bending.¹² The variations in initial E_f are believed due to variations in Ga:As surface stoichiometry.¹³

We measured Ga:As ratios corresponding to reconstructions from (4×6) through *c*(2×8).¹³ For Au(Al) on three (one) *n*- and one (two) *p*-type surfaces, Fig. 1 shows an initial E_f range of 0.3 (0.2) eV but a final E_f spread of only 0.05 (0.12) eV after 20 Å deposition. Thus initial surface composition and reconstruction do not dominate the final metal/GaAs band bending. This does not preclude compositional effects on E_f caused by variations in Ga:As outdiffusion and resultant interface stoichiometry.⁴ Overall, Fig. 1 demonstrates that band bending and SBH's for metals on GaAs are in fact not constrained to a narrow band.

Interface optical emission reveals new metal- and As-related states as well as deep levels in the bulk. These interface and bulk features reflect major differences between LEC- and MBE-grown GaAs. Figure 2 depicts room-temperature, 1.0 kV (surface-sensitive)¹⁰ CL and PL (5145 Å) features of As-capped, clean, and metallized MBE-grown *n*-type GaAs(100) and bulk, LEC-grown (110) surfaces. The As-capped spectrum (a) shows an emission band at about 1.43 eV, which we attribute to a near band-gap (NBG) transition, and a broad emission band centered around 1.0 eV, which shows a shoulder at ~0.8 eV and which extends to 1.3 eV. With desorption of the As cap(b), the broad emission band at 1.0 eV sharpens and the NBG transition intensity increases. This last factor results from a decrease in band bending, which otherwise separates free electron-hole pairs and thereby reduces radiative recombination.¹⁰ The relatively weak peak feature remaining at 1.0 eV corresponds to bulk deep traps, as confirmed by PLS, and contrasts with the relatively intense CLS features at 0.8–1.0 eV observed for clean and at 0.75 eV for metallized, LEC-grown GaAs.¹⁰ Hence, the As cap is associated with deep gap states and a 0.8 eV emission which contribute to increased band bending. Au metallization of the uncapped (100) surface produces new deep level emission features at 0.8 and 1.26 eV and increases the band bending. The negative (c-b) difference at NBG energies corresponds to increased band bending, in agreement with E_f movements for Au in Fig. 1. The new 1.26 eV emission corresponds either to new states located 1.26 eV

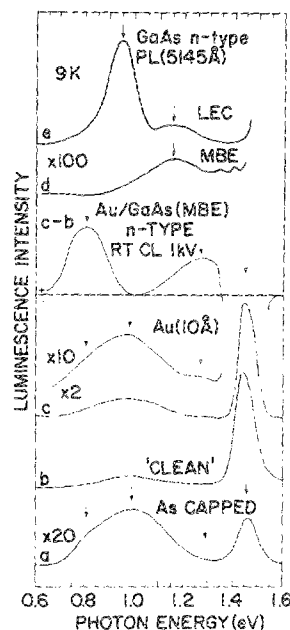


FIG. 2. Room-temperature CL spectra of (a) As-capped, (b) UHV-cleaned MBE-grown, *n*-type GaAs(100), (c) 10 Å deposited Au, (c-b) difference spectrum. PL spectra at 9 K of (d) MBE- and (e) LEC-grown *n*-type GaAs, $n = 5 \times 10^{17} \text{ cm}^{-3}$.

above the VB maximum or to transitions from the (CB) minimum to states at the Au/GaAs E_f position 1.23 ± 0.2 eV below. The new 0.8 eV emission resembles both the As-capped features as well as the dominant, LEC-grown native gap states, suggesting a common origin. The 9 K PL spectra in Fig. 2 (d,e) show that both materials contain deep levels, but that their densities are over two orders of magnitude higher for the LEC-grown GaAs. Moreover, the LEC peak distribution is shifted 0.2 eV closer to midgap, with the dominant 0.95 eV (0.86 eV at room temperature) peak close to the CLS emission for UHV-cleaned GaAs and close (e.g., 0.86 eV above the VB edge or below the CB edge) to the E_f stabilization energies reported previously.^{2,3} Conversely, the 1.15 eV peak (1.06 eV at room temperature) MBE-grown GaAs peak corresponds to the 1 eV CLS bulk peak in Fig. 2 but not to the E_f stabilization energies in Fig. 1. Thus, the densities and energies of deep levels evident in both bulk and surface-sensitive emission spectra are consistent with a stronger contribution of bulk traps to the E_f stabilization in LEC-grown GaAs.

The various factors which can contribute to the difference in MBE- versus melt-grown GaAs SBH ranges include surface crystallographic orientation,¹⁴ excess As,⁴ thermal pretreatment, and bulk traps. This last factor offers a relatively direct explanation consistent with the difference in interface states. Melt-grown GaAs contains high concentrations of deep levels, e.g., 2×10^{16} to $5 \times 10^{16} \text{ cm}^{-3}$ for LEC-grown¹⁵ and HB-grown¹⁵ material, respectively, far in excess of MBE-grown GaAs trap densities ($< 10^{13} \text{ cm}^{-3}$).¹⁷ LEC-grown crystals frequently contain native defects with the potential for electrical activity exceeding 10^{18} cm^{-3} , plus several electrically active deep levels with densities exceeding 10^{16} cm^{-3} which can segregate to the semiconductor

surface.¹⁹ When greater than the bulk doping, such interface traps can restrict E_f movement.²⁰ That such surface states are associated with crystalline defects in the surface space-charge region has already been suggested.²¹ Their origin may reside in the As-rich conditions under which they are grown^{15,16} and the deep levels produced thereby (Fig. 2).

Figure 1 shows that much better control of the interface properties is achieved in the metallization of MBE- versus LEC-grown GaAs. Furthermore, the band bending and interface state results impact several models of Schottky barrier formation. For melt-grown GaAs, the existence of high densities of states near midgap provides an explanation for the rapid E_f movements to a corresponding narrow energy range^{2,3} and preclude the need for chemisorption-induced states.^{2,3} On the other hand, discrete states due to As can act to screen charge transfer between metal and semiconductor and thereby limit E_f movement. The emission at ~ 0.75 eV¹⁰ lies almost exactly where expected from both work function as well as pinning properties, confirming the electrical activity long proposed by Woodall and Freeouf.⁴ The more intense CLS emission at this energy for melt-grown GaAs¹³ is consistent with its typical As-rich growth conditions. For MBE-grown GaAs, we obtain identical E_f stabilization positions for the same metals on both *n*- and *p*-GaAs, as expected from a self-consistent analysis of the junction electrostatics.²² Indeed, such an analysis reveals that the presence of a single acceptor state with surface density $3\text{--}5 \times 10^{13} \text{ cm}^{-2}$ at ~ 0.2 eV above the VB edge is compatible with the dependence of SBH on metal work function. The 1.26 eV Au-induced peak in Fig. 2 may correspond to a transition involving this state.

In conclusion, we have observed a broad range of Fermi level stabilizations at metal/MBE-grown GaAs(100) interfaces with almost identical *n*- and *p*-type E_f values. We observe optical emission from discrete, As-related as well as metal-specific interface states. Among potential factors producing the contrast between MBE- and melt-grown GaAs interface properties, the latter's higher bulk defect densities provide the most direct explanation, consistent with the differences in deep level interface emission and a self-consistent electrostatic analysis. Hence, the metal/MBE-grown GaAs results demonstrate that both chemical interactions and the quality of bulk crystal grown can play a major role for SB formation of III-V compound semiconductors.

Partial support by the Office of Naval Research (grant No. ONR N00014-80-C-0778), the Army Research Office (Contract DAAL03-86-C-003), and fruitful discussions with C.B. Duke are gratefully acknowledged. The Synchrotron Radiation Center, University of WI-Madison is supported by the National Science Foundation.

¹S. M. Sze, 2nd ed., *Physics of Semiconductor Devices* (Wiley-Interscience, New York, 1981), Chap. 5.

²W. E. Spicer, I. Lindau, P. Skeath, C. Y. Su, and P. Chye, *Phys. Rev. Lett.* **44**, 420 (1980); R. H. Williams, R. R. Varma, and V. Montgomery, *J. Vac. Sci. Technol.* **16**, 1418 (1979); R. Ludeke, T. C. Chiang, and T. Miller, *J. Vac. Sci. Technol. B* **1**, 581 (1983); M. Prietsch, M. Domke, C. Laubschat, and G. Kaindl, *Phys. Rev. Lett.* **60**, 436 (1988).

³N. Newman, W. E. Spicer, T. Kendelewicz, and I. Lindau, *J. Vac. Sci. Technol. B* **4**, 931 (1986).

⁴J. M. Woodall and J. L. Freeouf, *J. Vac. Sci. Technol.* **19**, 794 (1981); J. Freeouf and J. M. Woodall, *Appl. Phys. Lett.* **39**, 727 (1981).

⁵J. Tersoff, *Phys. Rev. B* **32**, 6968 (1985); W. Monch, *Phys. Rev. Lett.* **58**, 1360 (1987).

⁶R. Ludeke, D. Straub, F. J. Himpsel, and E. Landgren, *J. Vac. Sci. Technol. A* **4**, 874 (1986).

⁷L. J. Brillson, R. E. Viturro, M. L. Slade, P. Chiaradia, D. Kilday, M. K. Kelly, and G. Margaritondo, *Appl. Phys. Lett.* **50**, 1379 (1987).

⁸L. J. Brillson, M. L. Slade, R. E. Viturro, M. K. Kelly, N. Tache, G. Margaritondo, J. M. Woodall, P. D. Kirchner, G. D. Pettit, and S. L. Wright, *Appl. Phys. Lett.* **48**, 1458 (1986).

⁹L. J. Brillson, *Surf. Sci.* **51**, 45 (1975).

¹⁰R. E. Viturro, M. L. Slade, and L. J. Brillson, *Phys. Rev. Lett.* **57**, 487 (1986).

¹¹P. Chiaradia, A. D. Katnani, H. W. Sang, Jr., and R. S. Bauer, *Phys. Rev. Lett.* **52**, 1246 (1984).

¹²H. Brugger, F. Schaffler, and G. Arbreiter, *Phys. Rev. Lett.* **52**, 141 (1984).

¹³S. P. Svensson, J. Kanski, T. G. Andersson, and P. O. Nilsson, *J. Vac. Sci. Technol. B* **2**, 235 (1984); R. Z. Bachrach, R. S. Bauer, P. Chiaradia, and G. V. Hansson, *J. Vac. Sci. Technol.* **18**, 797 (1981).

¹⁴J. R. Waldrop, *Appl. Phys. Lett.* **44**, 1002 (1984). No significant difference between GaAs(100) and (110) is reported.

¹⁵D. E. Holmes, R. Y. Chen, K. R. Elliot, and C. G. Kirkpatrick, *Appl. Phys. Lett.* **40**, 46 (1982).

¹⁶J. Lagowski, H. C. Gatos, J. M. Parsey, K. Wada, M. Kaminska, and W. Walukiewicz, *Appl. Phys. Lett.* **40**, 342 (1982).

¹⁷A. Mircean and D. Bois, *Inst. Phys. Conf. Ser. No.* **46**, 82 (1979).

¹⁸I. Fujimoto, *Jpn. J. Appl. Phys.* **23**, L287 (1984).

¹⁹A. Yahata and M. Nakajima, *J. Appl. Phys.* **23**, L313 (1984).

²⁰A. Zur, T. C. McGill, and D. L. Smith, *Phys. Rev. B* **28**, 2060 (1983).

²¹T. M. Valahas, J. S. Sochanski, and H. C. Gatos, *Surf. Sci.* **26**, 41 (1971).

²²C. B. Duke and C. Mailhot, *J. Vac. Sci. Technol. B* **3**, 1170 (1985); *Phys. Rev. B* **33**, 1118 (1986).